

# Exclusive electroproduction of $K^+\Lambda$ and $K^+\Sigma^0$ final states at $Q^2 = 0.030\text{--}0.055$ (GeV/c)<sup>2</sup>

P. Achenbach<sup>1</sup>, C. Ayerbe Gayoso<sup>1</sup>, J.C. Bernauer<sup>1,6</sup>, S. Bianchin<sup>2</sup>, R. Böhm<sup>1</sup>, O. Borodina<sup>2</sup>, D. Bosnar<sup>3</sup>, M. Böss<sup>1</sup>, V. Bozkurt<sup>2</sup>, P. Bydžovský<sup>4</sup>, L. Debenjak<sup>5</sup>, M.O. Distler<sup>1</sup>, A. Esser<sup>1</sup>, I. Frišćić<sup>3</sup>, M. Gómez Rodríguez<sup>1</sup>, B. Göküzüm<sup>2</sup>, K. Griebinger<sup>1</sup>, P. Jennewein<sup>1</sup>, E. Kim<sup>2</sup>, M. Makek<sup>3</sup>, H. Merkel<sup>1</sup>, S. Minami<sup>2</sup>, U. Müller<sup>1</sup>, D. Nakajima<sup>2</sup>, L. Nungesser<sup>1</sup>, B. Özel-Tashenov<sup>2</sup>, J. Pochodzalla<sup>1</sup>, Ch. Rappold<sup>2</sup>, T. R. Saito<sup>1,2</sup>, S. Sánchez Majos<sup>1</sup>, B.S. Schlimme<sup>1</sup>, S. Širca<sup>5</sup>, M. Weinriefer<sup>1</sup>, and C.J. Yoon<sup>1,7</sup>

A1 Collaboration

<sup>1</sup> Institut für Kernphysik, Johannes Gutenberg-Universität, Mainz, Germany

<sup>2</sup> GSI, Helmholtz Center for Heavy Ion Research, Darmstadt, Germany

<sup>3</sup> Department of Physics, University of Zagreb, Croatia

<sup>4</sup> Nuclear Physics Institute, Řež near Prague, Czech Republic

<sup>5</sup> University of Ljubljana and Jožef Stefan Institute, Ljubljana, Slovenia

<sup>6</sup> *Present address:* MIT-LNS, Cambridge, MA, U.S.A.

<sup>7</sup> *Present address:* Department of Physics and Astronomy, Seoul National University, Korea

Received: date / Revised version: date

**Abstract.** Cross section measurements of the exclusive  $p(e, e' K^+) \Lambda, \Sigma^0$  electroproduction reactions have been performed at the Mainz Microtron MAMI in the A1 spectrometer facility using for the first time the KAOS spectrometer for kaon detection. These processes were studied in a kinematical region not covered by any previous experiment. The nucleon was probed in its third resonance region with virtual photons of low four-momenta,  $Q^2 = 0.030\text{--}0.055$  (GeV/c)<sup>2</sup>. The MAMI data indicate a smooth transition in  $Q^2$  from photoproduction to electroproduction cross sections. Comparison with predictions of effective Lagrangian models based on the isobar approach reveal that strong longitudinal couplings of the virtual photon to the  $N^*$  resonances can be excluded from these models.

## 1 Introduction

The Mainz Microtron MAMI at the Institut für Kernphysik in Mainz is an accelerator to study hadrons with the electromagnetic probe [1]. The exclusive production of mesons by electron and photon beams impinging on liquid hydrogen targets has been proven to be a valuable tool for investigating the hadronic structure of the nucleon. At the energy scale of the nucleon mass, hadrons are complex systems, whose description by fundamental equations for the dynamics of asymptotically free quarks and gluons is complicated by the non-perturbative nature of QCD. Instead, a successful description of these reactions has been obtained with hadronic field theories. The approach is based on effective degrees-of-freedom, where mesons and baryons are treated as fundamental objects which interact with one another, characterized by properties such as mass, charge, spin, parity, form factors, and coupling constants. Studies of strange final states provide additional information on the baryonic resonances.

In one particular type of effective Lagrangian model, commonly referred to as the isobar approach, the reaction amplitude is constructed in the lowest-order (tree level) assuming Born terms and exchanges of various nucleon, hyperon, and meson resonances in the  $s$ -,  $u$ -, and  $t$ -channels, respectively. Many such models use the single-channel approach, in which final-state interactions are neglected. Their copious applications into the strangeness sector started in the 1980s, e.g. [2,3,4,5,6]. For the elec-

---

*Correspondence to:* P. Achenbach, J.-J.-Becherweg 45, D-55099 Mainz, Germany, e-mail: [patrick@kph.uni-mainz.de](mailto:patrick@kph.uni-mainz.de)

tromagnetic kaon production in the so-called third resonance region, many resonances contribute, which presently cannot be described uniquely by a single model.

In the one-photon exchange approximation for electromagnetic scattering of unpolarized electrons off unpolarized target nucleons with coincident kaon detection the virtual photoproduction cross section can be expressed as

$$\frac{d\sigma_v}{d\Omega_K^{cm}} = \sigma_T + \varepsilon \sigma_L + \sqrt{2\varepsilon(\varepsilon+1)} \sigma_{TL} \cos \phi_K + \varepsilon \sigma_{TT} \cos 2\phi_K, \quad (1)$$

where the terms indexed by  $T$ ,  $L$ ,  $TL$ ,  $TT$  are the transverse, longitudinal and interference structure functions that depend on the virtual photon's four-momentum  $Q^2$  and the hadronic energy  $W$ , and  $\phi_K$  is the angle between the electron-scattering and hadron-production planes. This expression shows the close connection between electro- and photoproduction. At MAMI the transitional region at  $Q^2 < 0.5$  (GeV/c)<sup>2</sup> is accessible with virtual photons that are polarized with a degree-of-polarization  $\varepsilon$ . Longitudinal and longitudinal-transverse interference structure functions are accessible only in electroproduction experiments. Although not necessarily being small they are suppressed in the total cross section through a factor  $Q^2/\omega^2$ , with  $\omega$  being the photon energy. The  $\sigma_{TT}$  and  $\sigma_T$  structure functions are related to the polarized photon asymmetry  $\Sigma$ , that could be measured in photoproduction experiments with real polarized photons, by the relation  $\Sigma = -\sigma_{TT}(Q^2 \rightarrow 0)/\sigma_T(Q^2 \rightarrow 0)$ . The transverse-transverse interference structure function for virtual photons accounts for their partial linear polarization. With these connections it is instruc-

tive to compare the electroproduction cross section at very low  $Q^2$  directly to unpolarized photoproduction. For real unpolarized photons and unpolarized target nucleons only the transverse structure function remains.

In order to provide a comprehensive understanding of the elementary kaon production reaction, large kinematic coverage of experimental data on photo- and electroproduction is needed. Although recent electroproduction measurements with high statistics have been performed at Jefferson Lab [7, 8, 9, 10, 11], the region of very small momentum transfers was up to now not covered experimentally. A phenomenological extrapolation of the CLAS data from  $Q^2 > 0.65$  (GeV/c)<sup>2</sup> to the photoproduction point at  $Q^2 = 0$  leads to values of the transverse structure function  $\sigma_T$  systematically larger than the measured values in photoproduction [9]. This unknown transitional region is particularly interesting since predictions of models for the separated cross sections differ significantly here, see e.g. Fig. 3 in [10]. The goal of the first measurement at MAMI was to probe the elementary reaction at small momentum transfers and to determine the angular dependence of the electroproduction cross section in this kinematic region.

## 2 Experiment

First experiments on the electroproduction of kaons off a liquid hydrogen target were performed in Mainz with an unpolarized electron beam of 1.508 GeV energy in the years 2008–9. The liquid hydrogen target cell was 11 mm wide and 48 mm long with walls made of 10  $\mu\text{m}$  thick havar

foil. A current of 1–4  $\mu\text{A}$  was rastered with a few kHz in the transverse directions with an amplitude of  $\pm 5$  mm in order to avoid local boiling of the liquid. The scattered electrons from the  $p(e, e'K^+)$  reaction were detected in SpekB, one of the high-resolution magnetic spectrometers of the A1 collaboration's spectrometer facility [12], and the positive kaons in the KAOS spectrometer [13]. With its very compact design and a length of the central trajectory of only 5.3 m to the focal plane, the KAOS spectrometer complements the facility in reactions with open strangeness.

In two of the experimental settings, the central momentum for the kaon arm was 0.53 GeV/c and for the electron arm 0.33 GeV/c, respectively 0.45 GeV/c. The central spectrometer angle of the kaon arm was  $31.5^\circ$  with a large angular acceptance in the dispersive plane of  $\theta_K^{lab} = 21\text{--}43^\circ$ . The electron spectrometer was fixed at the minimum forward angle of  $\theta_e^{lab} \approx 15^\circ$ , thereby maximising the virtual photon flux. The coverage of the photon's four-momenta was  $Q^2 = 0.030\text{--}0.055$  (GeV/c)<sup>2</sup> with central values of  $Q^2 = 0.036$  and  $0.050$  (GeV/c)<sup>2</sup> for the two kinematic settings. The corresponding degrees-of-polarization were  $\varepsilon = 0.4$  and  $0.54$ . Photon energies,  $\omega$ , were near the maximum of the kaon production cross section at 1.18 GeV and 1.04 GeV, exciting the hadronic system to invariant energies  $W = 1.75$  GeV and 1.67 GeV.

Track determination is performed in SpekB by means of two vertical drift chambers, and timing and trigger signals are provided by two segmented planes of plastic scintillators immediately behind. A gas-filled threshold

Cherenkov detector is operated to provide a good separation between pions and electrons. To perform clean electron identification, a signal in the Cherenkov counter was required. SpekB reaches a momentum resolution (FWHM) of  $\delta p/p < 10^{-4}$  and an angular resolution of better than 0.2 mrad.

In the KAOS spectrometer's hadron arm there are two segmented scintillator walls with 30 paddles each serving as timing, energy loss, and trigger detectors. Two multi-wire proportional chambers serve as coordinate detectors near the focal plane. A dedicated set of efficiency counters was built to measure tracking efficiencies for the abundant pions and protons. The relatively large overlap between the liberated charges for these two particle species was used to extract the tracking efficiency for kaons.

The intrinsic efficiency of a single MWPC was measured to be better than 98%. Track reconstruction efficiencies were dependent on beam intensity, being 75–90% at beam currents of 1–4  $\mu\text{A}$  [14]. To identify kaons in the measured range of momenta from 0.4 to 0.7 GeV/c, energy loss and flight time were used. The signal amplitudes from the individual paddles were corrected for the reconstructed path length through the scintillator bulk material and the light absorption inside. The specific energy loss corrected for the expected kaon energy loss,  $\Delta E^K$ , was required to be within  $|\Delta E^K| < 640$  keV. See Fig. 1 for the measured specific energy loss in one scintillator wall as a function of momentum after particle identification cuts. The coincidence time spectra after particle identification cuts for the  $p(e, e'K^+)$  and  $p(e, e'\pi^+)$  reactions are shown in Fig. 2,

where the coincidence time was determined by using the reconstructed momentum and path length under the assumption that a kaon or pion was detected. The flight time corrected for the expected kaon flight time,  $\Delta t^K$ , was required to be within  $|\Delta t^K| < 1.2$  ns. The hadron arm trigger was generated by a combination of the hits in the two scintillator walls. Since the KAOS spectrometer was operated as a single dipole with open yoke geometry, a study was performed on the contributions from coincident particles originating outside the spectrometer acceptance that scattered into the detectors. These type of events were eliminated by the tracking cuts.

The measured momenta of the kaon and the electron allow for a full reconstruction of the missing energy and missing momentum of the recoiling system. The missing mass spectrum of one data set is shown in Fig. 3 with the mass resolution being sufficient to clearly separate  $\Lambda$  from  $\Sigma$  hyperons as the unobserved baryon in the reaction. Random background events, identified by two averaged  $(e', K^+)$  coincidence time sidebands and  $\sim 10\%$  of coincidence background, were subtracted with the appropriate weights. The mass resolution was limited by the uncertainties in the transfer matrix. For the  $\Lambda$  hyperons, events were selected in the range  $1.110 < M_X$  [GeV/c<sup>2</sup>]  $< 1.140$ , and for the  $\Sigma^0$  hyperons, events were selected in the range  $1.185 < M_X$  [GeV/c<sup>2</sup>]  $< 1.220$ .

### 3 Cross Sections

The experimental kaon yield,  $Y_K$ , in the two channels can be related to the cross section by

$$Y_K = \int \mathcal{L} dt \times \frac{d\sigma_v}{d\Omega_K^{cm}} \times \int \Gamma(Q^2, W) f(Q^2, W) A R dV, \quad (2)$$

where  $\Gamma$  is dependent on purely electromagnetic properties and can be considered as a “flux of virtual photons”, so that the virtual photoproduction cross section,  $\sigma_v$ , could be extracted.  $\mathcal{L}$  is the experimental luminosity that includes global efficiencies such as dead-times and beam current dependent corrections such as the tracking efficiency.  $A$  is the acceptance function of the coincidence spectrometer setup,  $R$  is the correction due to radiative and energy losses, and  $dV$  the phase-space element. The accumulated and corrected luminosity in 2009 was  $\int \mathcal{L} dt \sim 2300 \text{ fbarn}^{-1}$ . The kaon sample collected in 2008 was significantly smaller. In a Monte Carlo simulation of the experiment, the phase-space integral was evaluated in the volume  $\Delta V = \Delta Q^2 \Delta W \Delta \phi_K \Delta \Omega_K^{cm}$  with limits that extended beyond the physical acceptances of the spectrometers. Radiative corrections in  $R$  were included according to [15]. The solid angle acceptances for the electrons and kaons in the laboratory system were  $\Omega_e^{lab} = 5.6 \text{ msr}$  and  $\Omega_K^{lab} = 10.4 \text{ msr}$ . The two different kaon momenta associated to  $\Lambda$  and  $\Sigma^0$  hyperons were simultaneously within the momentum acceptance of the KAOS spectrometer.

The geometrical acceptance of the spectrometer setup, the path length from the target to the detectors, kaon decay in flight, and kaon multiple scattering were deter-

mined using the simulation package Geant4. The kaon survival fraction varied between 0.2 and 0.35 for the range of momenta detected. Fiducial cuts were applied in target acceptance to restrict events to a region where agreement between the Monte Carlo code and the analysed data was excellent.

To study the dependence of the measured cross section on the kaon center-of-mass (cm) angle,  $\cos \theta_K^{cm}$ , the data was scaled to the center of the electron-arm acceptance, through the introduction of a scaling function  $f(Q^2, W)$  inside the phase-space integral. The scaling minimized the effects of non-uniform distribution within the  $W$  and  $Q^2$  bins and the extracted cross sections can be accurately compared directly to theoretical calculations at the center of each bin value. The scaling was performed with the predictions from isobaric models, see next Section for their description. The magnitude of the scaling varied between 0.85 and 1.15 with most of the events being scaled by less than 5%. The studied isobar models predicted only small variations of the scaling function. The model dependence and the uncertainty introduced by the scaling were included in the estimate of the systematic uncertainties.

At each kinematic setting, data were partitioned into several runs. The run-to-run variation of quantities like dead-time, background particle yields, etc. was used as a consistency check. The systematic uncertainty assigned to the absolute cross sections is 8% and is dominated by the uncertainties in KAOS acceptance (5%), MWPC tracking efficiencies (4%), analysis cut efficiencies (3%) and scaling model variation (2%). The beam current was measured

on the 1% level. Other studied sources of systematic uncertainties included kaon survival probability, kaon decay particle mis-identification, effective target length and target density fluctuations that introduced a systematic uncertainty on the percent level. These uncertainties are significantly smaller than the statistical uncertainties in the range of 10–25%.

The elementary kaon electroproduction cross section was measured at MAMI in a kinematic region of low  $Q^2$  not covered by previous experiments. The measured angular differential cross sections at  $W = 1.75$  GeV and  $\langle Q^2 \rangle = 0.036$  (GeV/c)<sup>2</sup> in the  $K^+\Lambda$  and  $K^+\Sigma^0$  reaction channels are shown in Fig. 4. The magnitude of the cross section is comparable to photoproduction data from the SAPHIR [16] and CLAS [8,11] measurements. Its angular dependence is almost flat in the  $K^+\Sigma^0$  channel whereas in the  $K^+\Lambda$  channel the data reveals a moderate angular dependence, which is consistent with the photoproduction data and with conclusions drawn from the CLAS electroproduction data [9]. In Fig. 5 the differential cross section at larger momentum transfer  $\langle Q^2 \rangle = 0.05$  (GeV/c)<sup>2</sup> and smaller hadronic energy  $\langle W \rangle = 1.67$  GeV in the  $K\Lambda$  channel is shown.

The MAMI cross section data in the two hyperon channels is also compared to predictions from variants of the K-Maid model [6] and from the Saclay-Lyon model [4]. The K-Maid model includes the kaon resonances  $K^*(890)$  and  $K_1(1270)$  in the  $t$ -channel, as well as four nucleon resonances,  $S_{11}(1650)$ ,  $P_{11}(1710)$ ,  $P_{13}(1720)$ , and a less well known spin-3/2 and isospin-1/2 resonance near 1.9 GeV

that is found within the context of this model to contribute in the  $s$ -channel of the  $K^+\Lambda$  production. For  $K^+\Sigma$  production the latter is replaced by the  $S_{31}(1900)$  and  $P_{31}(1910)$   $\Delta$ -resonances. Phenomenological form factors are used at the hadron vertices to account for the high energy region behaviour at  $W > 1.9$  GeV. No hyperon resonances are used in this model. Coupling constants are obliged to fulfill the constraints given by the 20% broken  $SU(3)$  symmetry. An interactive version of the model is available through the internet [6] and is referred to in this letter as the original variant. The parameters of the model, which are necessary to extend the model to the electroproduction process, e.g. the longitudinal coupling constants, were fitted using the  $Q^2$  dependence between 0.52 and 2.0 (GeV/c)<sup>2</sup> of the longitudinal and transverse cross sections measured at Jefferson Lab [17]. Another variant of the model has been constructed, in which the strong longitudinal couplings to  $N^*$  resonances were removed. This resulted in much smaller longitudinal contributions. In the variant labelled P<sub>1720</sub> only the longitudinal coupling to the  $P_{13}(1720)$  nucleon resonance has been removed. Further, some inconsistencies in the convention for the amplitudes, in the electromagnetic form factors in the Born terms, and in the couplings to spin-3/2 resonances have been corrected, resulting in minor changes to the predictions. This variant is referred to in this letter as the reduced variant. Finally, a new version of K-Maid is under construction, that uses very small longitudinal couplings [18]. In this version four nucleon resonances,  $D_{15}(1675)$ ,  $D_{13}(1700)$ ,  $F_{15}(2000)$ , and  $D_{15}(2200)$  were added to those assumed in

the original version and the free parameters of the model were re-fitted to describe the new world data on the photo- and electroproduction of kaons. This version is referred to as the extended variant.

The version of the Saclay-Lyon model used in the description of the data shares with K-Maid the same kaon resonances and the  $SU(3)$  constraints on the main coupling constants. The set of nucleon resonances differs from K-Maid and includes resonances with spins up to  $5/2$ , see [4]. Instead of hadronic form factors the spin- $1/2$  hyperon resonances  $S_{01}(1405)$ ,  $P_{11}(1660)$ ,  $S_{01}(1670)$  and  $P_{01}(1810)$  are used for counterbalancing the strength of the Born terms through a destructive interference with these  $u$ -channel resonances. For  $K^+\Sigma^0$  production, the  $P_{33}(1232)$ ,  $P_{31}(1910)$ , and  $P_{33}(1920)$   $\Delta$ -resonances are added to those given above.

## 4 Discussion

The observed behaviour of the cross section in the vicinity of the photoproduction point is very important for understanding dynamics of the process.

The MAMI data indicate a smooth transition in  $Q^2$  from photoproduction to electroproduction cross sections for both reaction channels as shown in Fig. 6. The CLAS data on the unpolarized cross section in the  $K^+\Lambda$  channel, measured for  $0.65 < Q^2 < 2.5$  (GeV/c)<sup>2</sup>, reveals a fall-off with respect to the photoproduction point [9]. However, the extrapolation of this trend to the photoproduction point with a dipole form results in a too large structure function  $\sigma_T$  [9], which is apparent especially at forward

kaon angles. These observations suggest a more complex dynamics of the  $K^+\Lambda$  electroproduction process in the transition region of  $0 < Q^2 < 0.5$  (GeV/c)<sup>2</sup>. Moreover, various models have predicted different transitions between the photoproduction point and the electroproduction cross section.

Information could also be obtained on the electromagnetic couplings to hadronic resonances. In Fig. 7 separated cross sections from the original K-Maid model are compared to the MAMI data which covers a range in  $Q^2$  from 0.030 to 0.055 (GeV/c)<sup>2</sup>. It was predicted that the longitudinal contribution exceeded the transverse cross section which was explained in the model by a strong longitudinal coupling of the electromagnetic field to the resonances. These couplings are given in the Lagrangian at the nucleon–photon–resonance vertices by a term that is proportional to  $Q^2$ . This effect is apparent especially in Fig. 7 at  $W = 1.67$  GeV where the steep rise of the longitudinal cross sections is due to the contribution from a strong longitudinal coupling of the resonance  $P_{13}(1720)$ . In contrast, models without longitudinal couplings predicted the electroproduction cross sections below the photoproduction data, which means that in these variants the total cross section slowly varied with  $Q^2$ . Also, the extended variant of the K-Maid model reveals a rather flat  $Q^2$  dependence of the cross section in both channels.

This first open strangeness experiment has also demonstrated that the KAOS spectrometer is, in connection with the high-quality continuous wave electron beam of MAMI, a very effective tool for investigating kaon production off

nucleons and nuclei with electron scattering. Based on the MAMI data some versions of isobar models for the process, which assumed strong longitudinal couplings to the nucleon resonances, could be excluded at the low energies that were probed. Other versions of isobar models, in which weak or no longitudinal couplings to  $N^*$  resonances appear, predict much smaller total cross sections and are in better agreement with the data. At MAMI, new measurements at very low  $Q^2$  with polarized beam will provide more complete information on the longitudinal-transverse response in this process and therefore will deliver additional new constraints on the model parameters.

To conclude, this measurement and expected new data from MAMI in this kinematic region will help in better understanding the dynamics of the electromagnetic kaon production and in the modeling of the nucleon and its resonances.

We would like to thank the accelerator group of MAMI and the staff of the workshops for their excellent support. We are thankful to T. Mart from the University of Indonesia for providing the K-Maid code and who assisted in the interpretation of the model. We also thank Th. Walcher and A. Jankowiak for their support in the early phase of the project.

Work supported in part by the Federal State of Rhineland-Palatinate and by the Deutsche Forschungsgemeinschaft (DFG) with the Collaborative Research Center 443, by the Research Center “Elementary Forces and Mathematical Foundations”, and by the DFG with the HBF-122-572 grant. We also acknowledge the support by the Research Infrastructure Integrating Activity “Study of Strongly Interacting Matter Hadron-

Physics2 under the 7th Framework Programme of EU and by the Grant Agency of the Czech Republic, grant No. 202/08/0984.

## References

1. K.H. Kaiser et al., Nucl. Instr. Meth. Phys. Res. **A 593**, 159 (2008)
2. R.A. Adelseck, B. Saghai, Phys. Rev. **C 42**, 108 (1990)
3. R.A. Williams, C.R. Ji, S.R. Cotanch, Phys. Rev. **C 46**, 1617 (1992)
4. J.C. David, C. Fayard, G.H. Lamot, B. Saghai, Phys. Rev. **C 53**, 2613 (1996)
5. T. Mizutani, C. Fayard, G.H. Lamot, B. Saghai, Phys. Rev. **C 58**, 75 (1998)
6. T. Mart, C. Bennhold, Phys. Rev. **C 61**, 012201 (2000), t. Mart, C. Bennhold, H. Haberzettl, L. Tiator, An effective Lagrangian model for kaon photo- and electroproduction on the nucleon, online available at [www.kph.uni-mainz.de/MAID/kaon/kaonmaid.html](http://www.kph.uni-mainz.de/MAID/kaon/kaonmaid.html)
7. R.M. Mohring et al. (E93-018 Collaboration), Phys. Rev. **C 67**, 055205 (2003)
8. R. Bradford et al. (CLAS Collaboration), Phys. Rev. **C 73**, 035202 (2006)
9. P. Ambrozewicz et al. (CLAS Collaboration), Phys. Rev. **C 75**, 045203 (2007)
10. M. Coman et al. (Jefferson Lab Hall A Collaboration), Phys. Rev. **C 81**, 052201 (2010)
11. M.E. McCracken et al. (CLAS Collaboration), Phys. Rev. **C 81**, 025201 (2010)
12. K.I. Blomqvist et al. (A1 Collaboration), Nucl. Instr. and Meth. Phys. Res. **A 403**, 263 (1998)
13. P. Achenbach et al. (A1 Collaboration), Eur. Phys. J. Special Topics **198**, 307 (2011)

14. P. Achenbach et al. (A1 Collaboration), Nucl. Instr. Meth. Phys. Res. **A 641**, 105 (2011)
15. L.W. Mo, Y.S. Tsai, Rev. Mod. Phys. **41**, 205 (1969)
16. K.H. Glander et al. (SAPHIR Collaboration), Eur. Phys. J. **A 19**, 251 (2004)
17. G. Niculescu et al. (E93-018 Collaboration), Phys. Rev. Lett. **81**, 1805 (1998)
18. T. Mart, L. Tiator (2011), private communication, to be published.

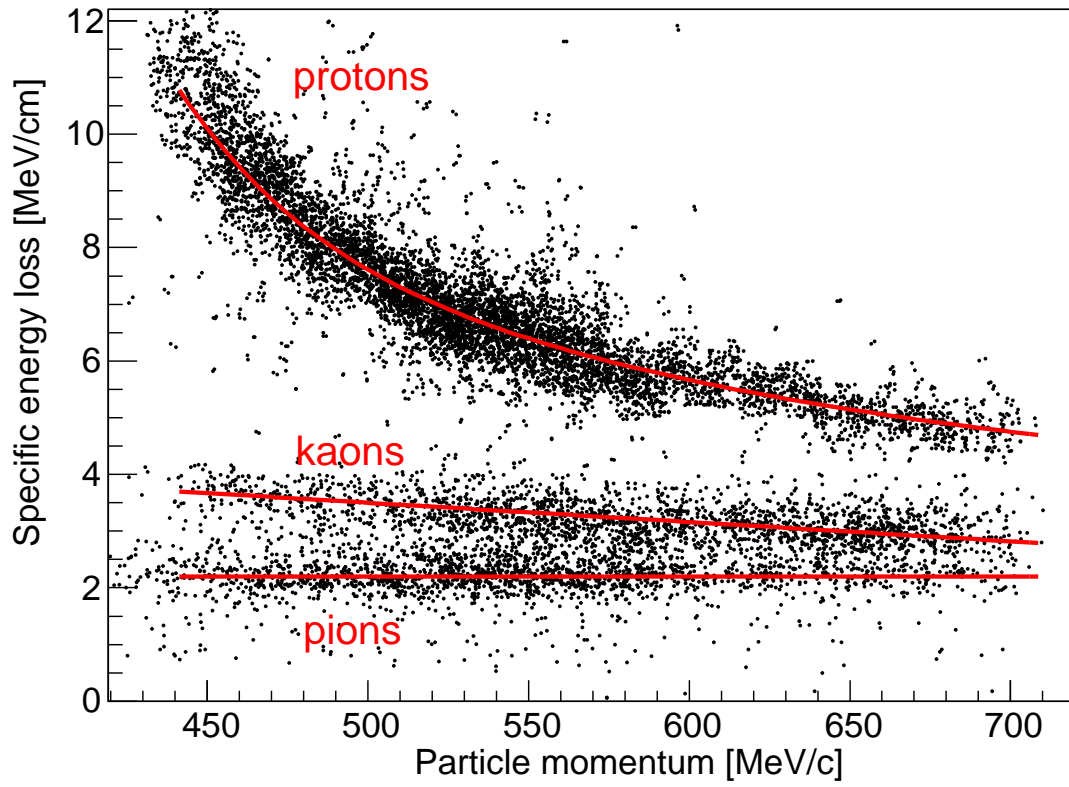


**Fig. 1.** Specific energy loss in one scintillator wall as a function of momentum after particle identification cuts. Lines for the expected energy losses of pions, kaons, and protons are shown.

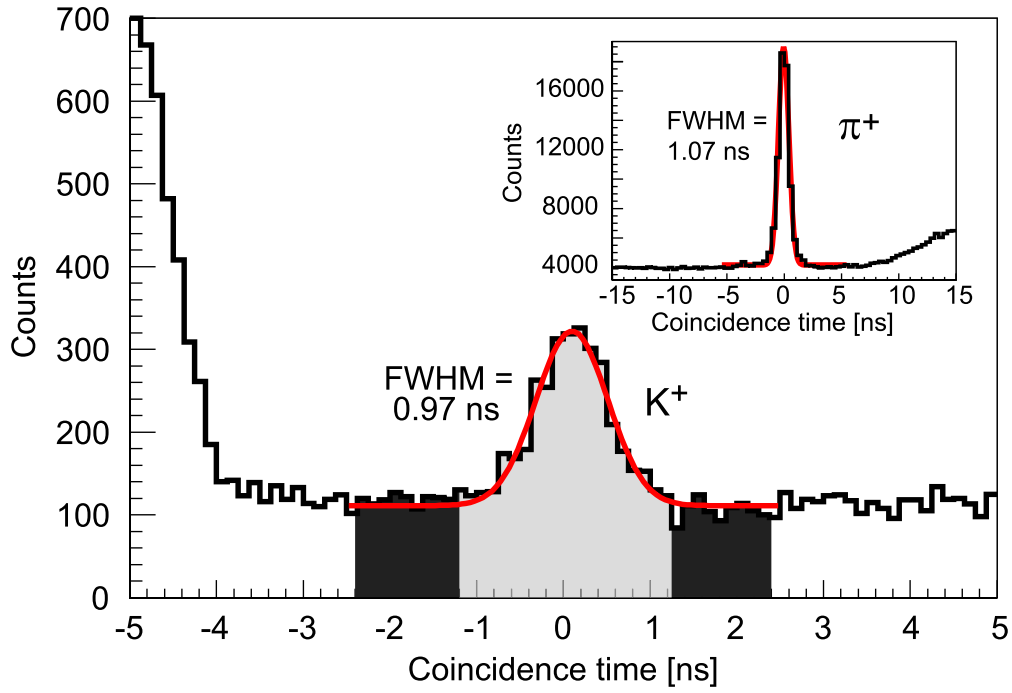


**Fig. 2.** Coincidence time spectra for the  $p(e, e'K^+)$  reaction as well as for the dominant  $p(e, e'\pi^+)$  reaction (insert), after corrections for the reconstructed flight path and particle identification cuts. Gaussian distributions on top of a constant background were fitted to the spectra. The width of the  $(e', \pi^+)$  peak is  $\Delta t_{FWHM} = 1.07$  ns, the width of the  $(e', K^+)$  peak is  $\Delta t_{FWHM} = 0.97$  ns. The cut regions for selecting true and random coincidences of kaons are indicated.

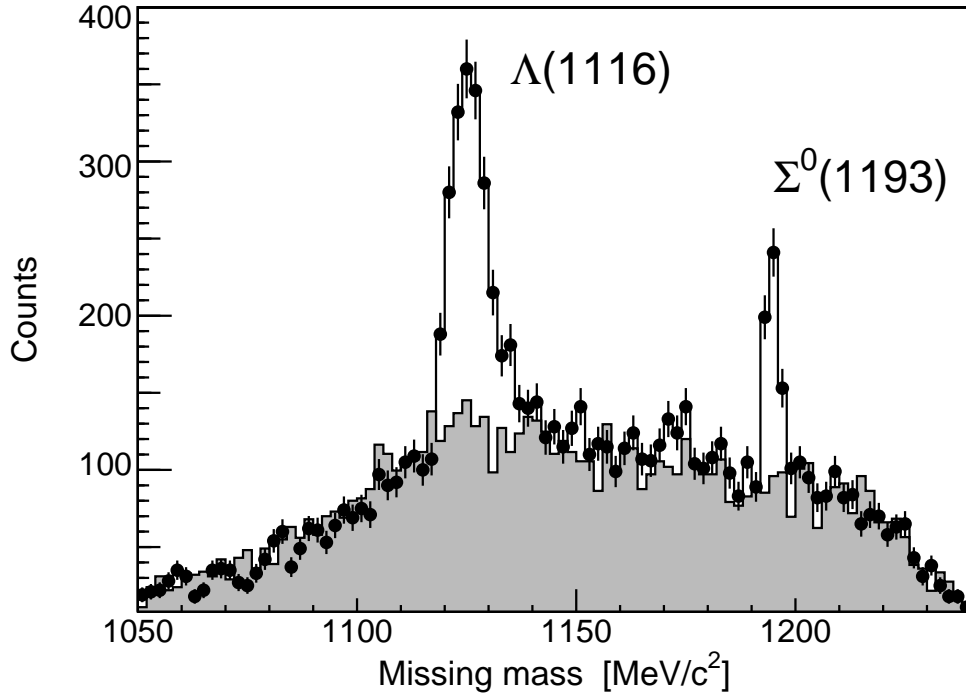


**Fig. 3.** Missing mass spectrum in the  $p(e, e'K^+)\Lambda, \Sigma^0$  reaction for one data set. The shaded histogram shows the missing mass distribution in two averaged  $(e', K^+)$  coincidence time sidebands with the appropriate weights and  $\sim 10\%$  of coincident background.

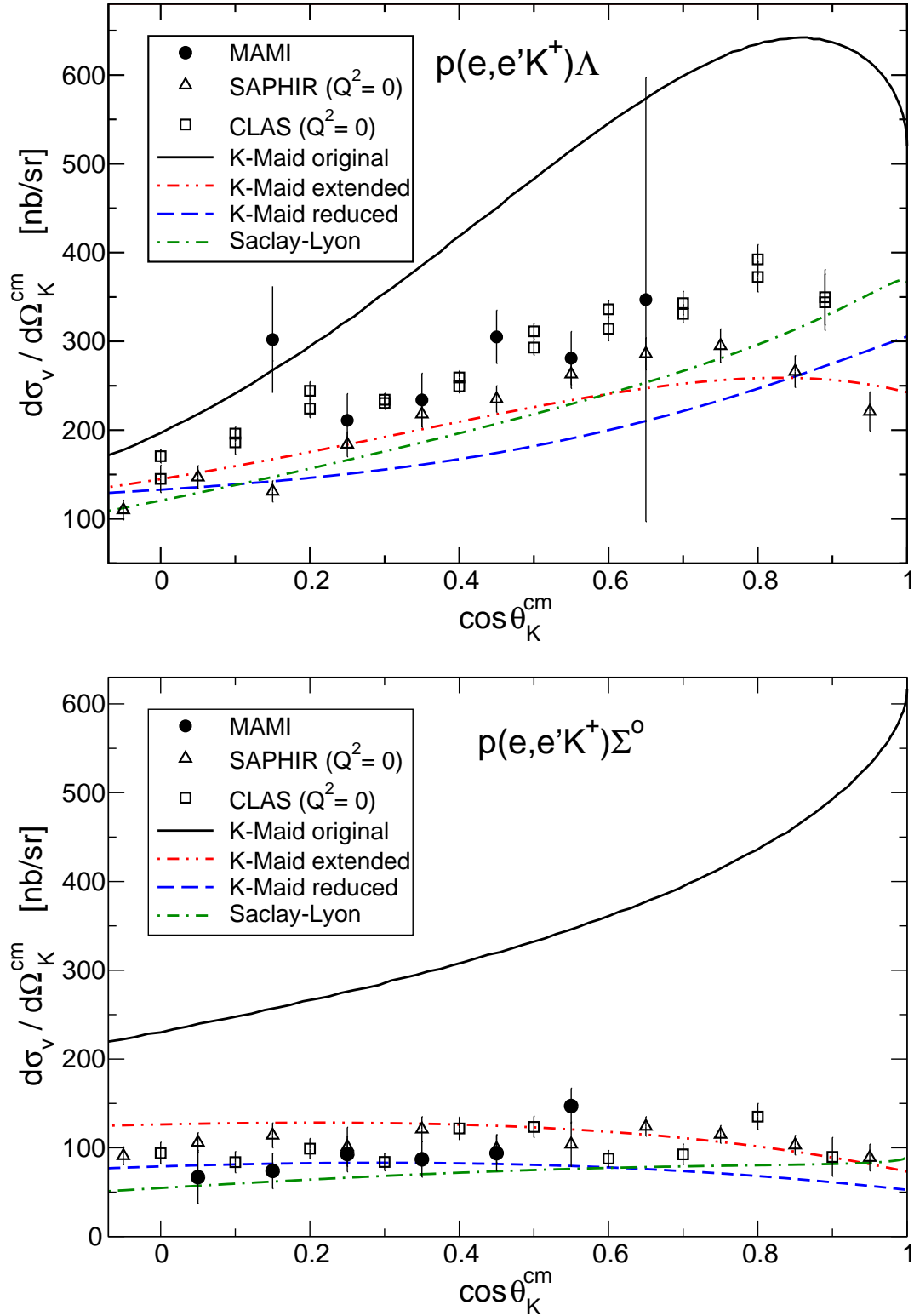


**Fig. 4.** Differential cross sections of kaon electroproduction scaled to the center of the experimental acceptance at  $\langle Q^2 \rangle = 0.036$  (GeV/c)<sup>2</sup>,  $\langle W \rangle = 1.75$  GeV and  $\langle \varepsilon \rangle = 0.4$ . The MAMI data is compared to variants of the K-Maid model [6] (see the text for discussion on the variations) and the Saclay-Lyon model [4]. The model predictions were averaged in  $Q^2$  between  $0.030\text{--}0.045$  (GeV/c)<sup>2</sup> and in  $W$  between  $1.74\text{--}1.76$  GeV. The photoproduction cross sections at  $Q^2 = 0$  are from the SAPHIR experiment at  $W = 1.757$  GeV [16] and from the CLAS experiment at  $W = 1.745\text{--}1.755$  GeV [8, 11].

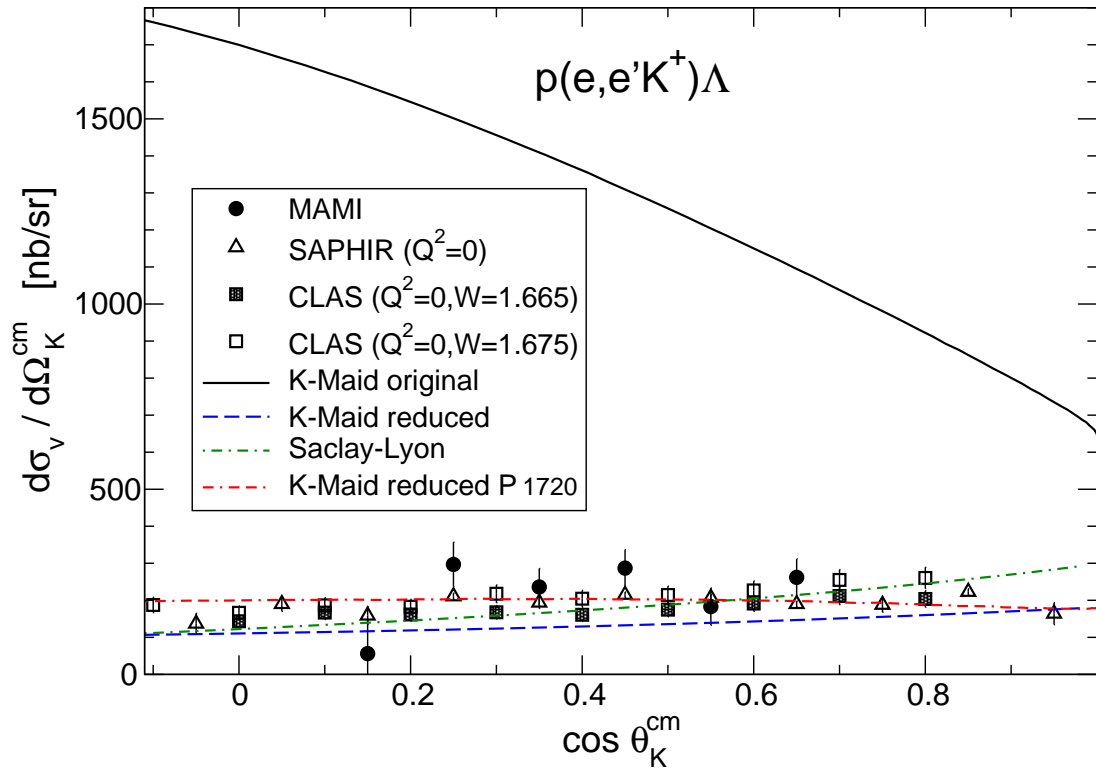


**Fig. 5.** Differential cross sections of kaon electroproduction scaled to the center of the experimental acceptance at  $\langle Q^2 \rangle = 0.05$  (GeV/c) $^2$ ,  $\langle W \rangle = 1.67$  GeV and  $\langle \varepsilon \rangle = 0.54$ . The data is compared to variants of the K-Maid model [6] (see the text for discussion on the variations) and the Saclay-Lyon model [4]. The photoproduction cross sections at  $Q^2 = 0$  are from the SAPHIR experiment [16] and from the CLAS experiment at  $W = 1.665$  and  $1.675$  GeV [8,11].

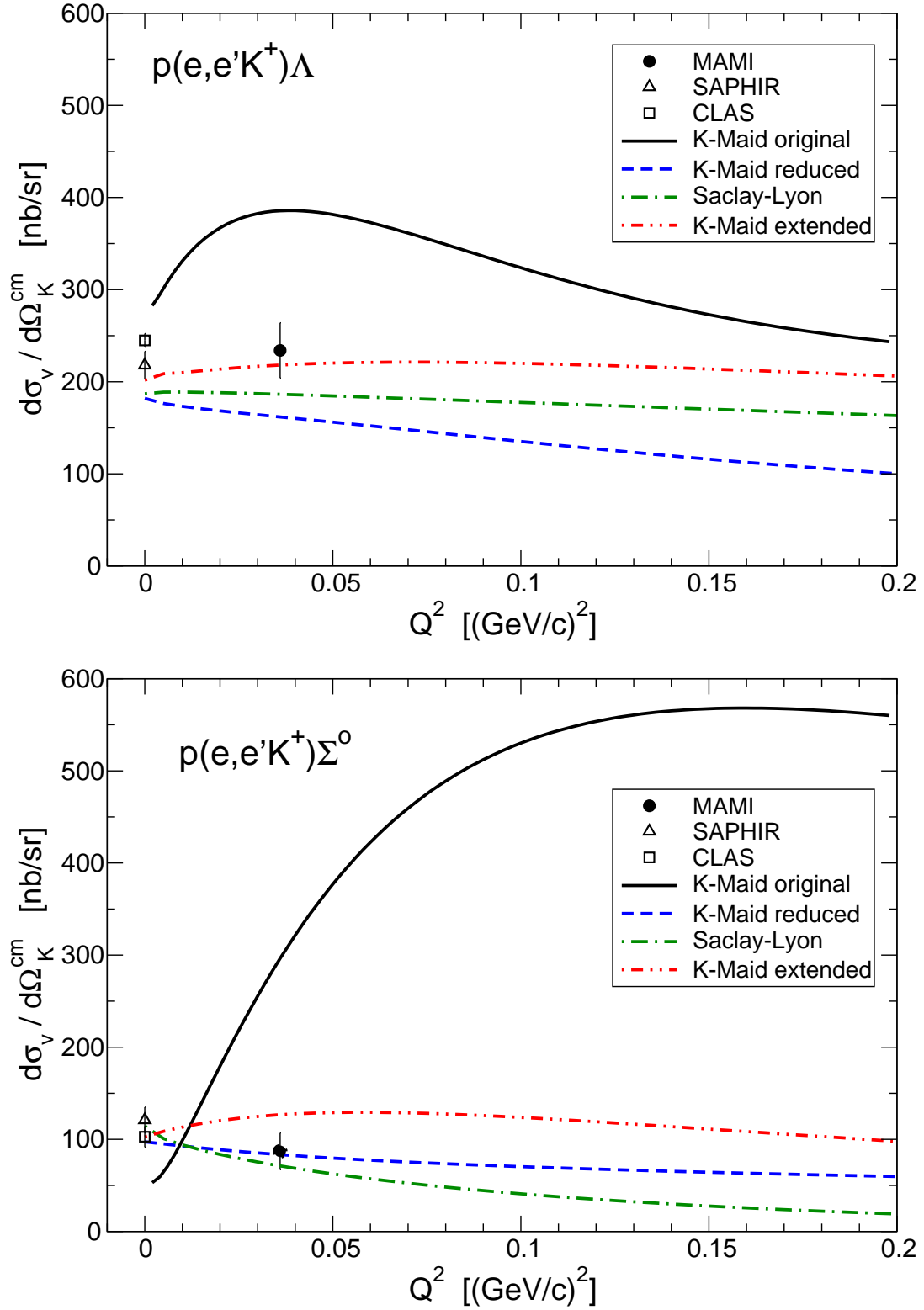


**Fig. 6.** Predictions for the dependence of the kaon electroproduction cross sections on the virtual photon's four-momentum  $Q^2$  at  $\cos\theta_K^{cm} = 0.35$  compared to the two experimental data points from MAMI for the  $K^+\Lambda$  and  $K^+\Sigma^0$  reaction channels.

References for models and data are the same as for Fig. 4.

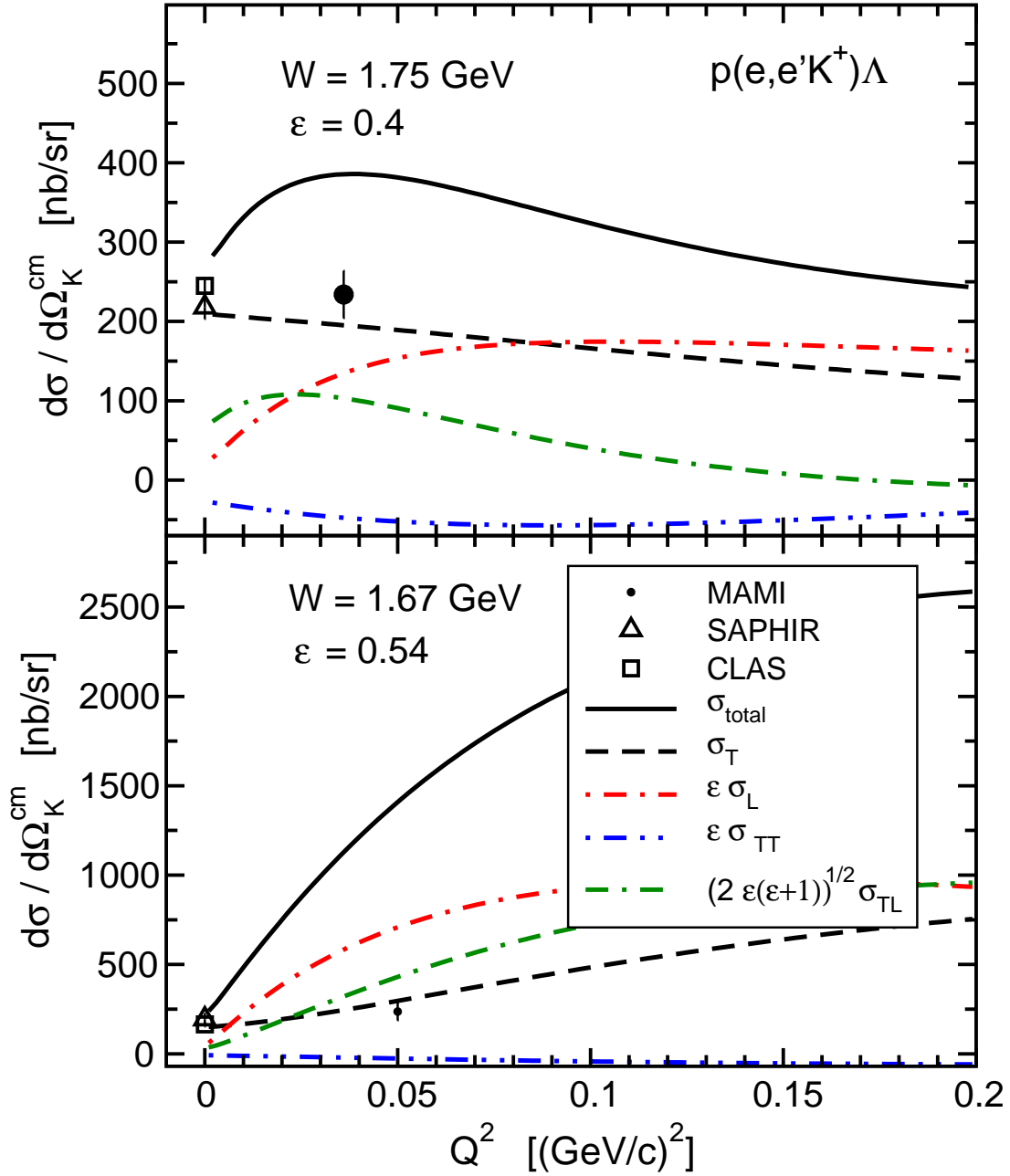


**Fig. 7.** Predictions from the original K-Maid model for the dependence of the kaon electroproduction cross sections on  $Q^2$  at  $\cos \theta_K^{cm} = 0.35$ , separated according to Eq. 1, compared to the data from MAMI for the  $K^+\Lambda$  reaction channel. A strong rise with  $Q^2$  of the longitudinal,  $\sigma_L$ , and the transverse-longitudinal interference,  $\sigma_{TL}$ , structure functions was predicted by the model, especially at  $W = 1.67$  GeV where the influence of a strong longitudinal coupling of the resonance  $P_{13}(1720)$  is apparent. In contrast, the transverse structure function,  $\sigma_T$ , is only slowly varying with  $Q^2$ . References for model and data are the same as for Fig. 4.